Optik xxx (2014) xxx–xxx

Contents lists available at ScienceDirect

Optik

journal homepage: www.elsevier.de/ijleo

All optical SRR switch using carbon nanotube composite

Davood Fathi*, Maryam Sakhdari, Mehdi Hajizadegan

School of Electrical and Computer Engineering, Tarbiat Modares University (TMU), Tehran 14115-194, Iran

ARTICLE INFO

Article history:
Received 11 August 2013
Accepted 20 February 2014
Available online xxx

Keywords:
All optical SRR switch
CNT composite
Nonlinear effects
Metamaterial

ABSTRACT

This paper presents a new design for all optical SRR metamaterial switch with carbon nanotube (CNT) composite as the nonlinear layer. Because of strong nonlinear effects of CNT composite layer, a low threshold power pump for switching is achieved. The possible fabrication of CNT composite besides the tunable applied frequency, are the main advantages of new designed structure.

1. Introduction

Metamaterials with unavailable optical properties in nature such as the negative refraction, have been studied extensively from optical to microwave frequency ranges [1]. They show a wide range of new applications such as sub wavelength image [2], slow light and cloaking [3]. In many cases, metallic resonators such as split ring resonators (SRRs) and fishnet structures are used to demonstrate the negative index metamaterial [4,5].

The design of all optical switches based on SRRs has attracted a great deal of attention in recent years, however only a limited number of materials have been used in their design and fabrication. For example, Chen et al. [6] have proposed a structure for terahertz electro optical switch based on SRRs and Gong et al. [7] have investigated theoretically an all optical absorption switch using an effective medium which its strong Kerr nonlinear effect has been discussed in [8].

Since their discovery in 1991 by Ijima [9], CNTs have found practical applications in several fields. It is well known that, materials with large third order optical nonlinearities are required for photonic applications including all optical switching, data processing, eye and sensor protection. Due to superior electrical and optical characteristics, the CNT structures and composites have been attracted by the researchers for using in electrical and optical devices [10–15]. Also the optical switching properties of CNT composites have been discussed in [16]. But all optical metamaterial switch structure based on the Kerr effect of CNT composite which is presented and discussed in this paper is a new idea which has not been introduced before.

The strong third order optical nonlinearity of CNT-paraffin composite provides it as a good candidate for nonlinear optical applications. CNTs have third order susceptibility (χ^3) dependent on the nanotube radius. In order to prevent the inter-band absorption and achieve a transparent region for the CNT composite, there is a low frequency limit where the incident photon energies satisfy the condition $\hbar\omega_i << \varepsilon_g$. For the case of CNT-paraffin composite, the imaginary part of $\chi^{(3)}$ is equal to zero and thus no inter-band absorption is occurred, whereas its real part is obtained about 10^{-7} esu [17]. This value is appropriate for practical applications in nonlinear optical devices.

In this paper, we introduce a novel structure for all optical SRR switch based on metamaterial which the CNT composite has been used as the nonlinear layer. For the three-dimensional simulation of switching performance we need to have the optical parameters of CNT composite layer. In [18], the permittivity dispersion of single wall CNT (SWCNT) has been calculated using some experimental results for the grapheme permittivity. Here we combine some methods to calculate theoretically the effective parameters from experimentally verified references. In addition, two kinds of nonlinear layer including CNT-paraffin and CNT-$BaTiO_3$ have been implemented and studied in the structure, which latter choice has a higher third order nonlinear susceptibility than former one [19]. So our work is a combination of several efforts such as the calculation of effective parameters for MWCNT and MWCNT composite, the structure design for an all optical switch and the simulation of switching performance.

* Corresponding author. Tel.: +98 21 82884973; fax: +98 21 82884325.
E-mail address: d.fathi@modares.ac.ir (D. Fathi).

http://dx.doi.org/10.1016/j.ijleo.2014.02.039
0030-4026/

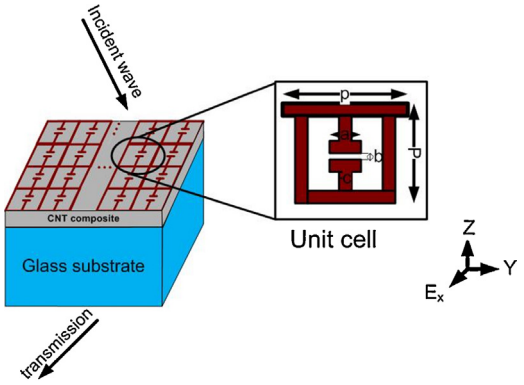

Fig. 1. The schematic of total structure and the related unit cell for the proposed all optical SRR switch, with $a = 10$, $b = 2$, $c = 4$ and $p = 50$ nm.

The paper is organized as follows: In Section 2, the proposed structure for the all optical SRR switch is introduced and discussed. Section 3 discusses about the effective optical parameters of CNT composite. Then in Section 4, the simulation results are presented. In this section, two cases for the nonlinear layer are considered: in one case, Paraffin has been used as the host media for the CNT composite, and in the other case, $BaTiO_3$ has been used. Finally in Section 5, the paper is concluded.

2. The proposed structure

Fig. 1 shows the schematic of total structure and the related unit cell for the proposed all optical SRR switch. The implemented unit cell in the structure is based on a recently presented electric analog to split ring resonators (SRRs) which consists of two single golden SRR put together on a split gap side [6–20]. In our proposed structure, this unit cell is placed on a CNT composite layer deposited on the glass substrate.

It should be noted that, the switch structure is illuminated from the top of it, as indicated in Fig. 1. The schematic of total structure and the related unit cell for the proposed all optical SRR switch, with $a = 10$, $b = 2$, $c = 4$ and $p = 50$ nm, and consequently the output wave as the switch response (transmission) will be obtained and detected by a detector placed under the switch structure.

Fig. 3 shows the equivalent circuit model for the split ring resonator (SRR) unit cell. A capacitor-like structure couples to the electric field and is connected in parallel with two loops, which each provides an inductance to the circuit model, as discussed in [21]. This configuration allows the electric field to drive the LC resonance providing both positive and negative electric polarizations at different frequencies along the resonance curve, where the phase of resonator response is in phase and out of phase with the driving field, respectively [20]. The two inductive loops are connected in parallel, so the equivalent inductance will be $L/2$. Now, the resonance frequency can be calculated as $\omega = \sqrt{2/(LC)}$. The resistance R in Fig. 2 models the dissipation in the golden split rings.

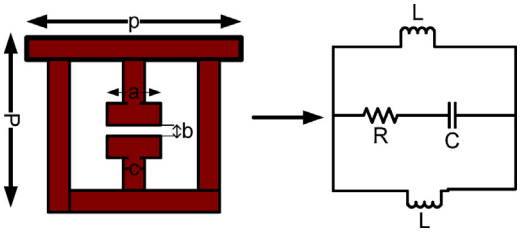

Fig. 2. The equivalent circuit model for the SRR unit cell.

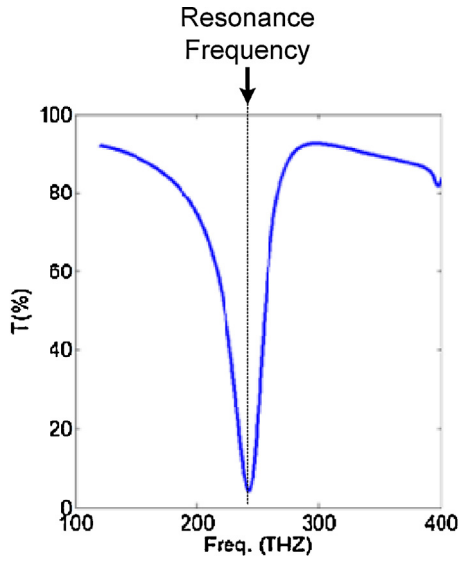

Fig. 3. The transmission coefficient versus the resonance frequency for the SRR unit cell.

Fig. 3 shows the transmission coefficient versus the frequency for the SRR unit cell with the geometric parameters as in Fig. 1. As it is clear, the transmission (output signal) falls to zero at the resonance frequency of about 240 THz, which is due to the impedance matching.

It should be noted that, in the proposed all optical switch, the probe signal is tuned on at the resonance frequency, so the output signal will be normally zero at this frequency. In this method, a high power pulse (pump) is used to change the switch state from off to on due to the nonlinear effects of CNT composite (Kerr effect) [22]. This subject will be discussed completely in Section 4.

3. The effective optical parameters of CNT composite

The widely used descriptions for the effective dielectric function are the Bruggeman and Maxwell–Garnett effective medium theory (EMT) [18,23]

$$\frac{f(\varepsilon_{CNT} - \varepsilon_{eff})}{\varepsilon_{eff} + L(\varepsilon_{CNT} - \varepsilon_{eff})} + \frac{(1-f)(\varepsilon_h - \varepsilon_{eff})}{\varepsilon_{eff} + L(\varepsilon_h - \varepsilon_{eff})} = 0 \quad (1)$$

$$\varepsilon_{eff_{\parallel}} = \varepsilon_h + f(\varepsilon_{\parallel} - \varepsilon_h) \quad (2)$$

$$\varepsilon_{eff\perp} = \varepsilon_h + \left[\frac{f(\varepsilon_{\perp} - \varepsilon_h)}{\varepsilon_h} + \left(\frac{1}{2}\right)(1-f)(\varepsilon_{\perp} - \varepsilon_h)\right] \quad (3)$$

where ε_{CNT} and ε_h are the complex dielectric constant of CNT and host material, respectively. Also ε_{eff} is the effective dielectric constant of CNT composite, f is the volume fraction of CNT contained in the composite, and L is the depolarization factor of each CNT in the composite.

3.1. CNT-paraffin composite

First we have used the vertical and parallel permittivities of graphite given in [24] for calculating the permittivity of MWCNT using Eq. (1) [25], then using Eqs. (2) and (3) we have calculated the effective permittivity of CNT-paraffin composite. Figs. 4 and 5 show the parallel and vertical effective permittivities of CNT-paraffin composite respectively, calculated using Eq. (1).

Figs. 6 and 7 show the effective parallel and vertical permittivities of CNT-paraffin composite respectively, which are calculated using Eqs. (2) and (3).

Please cite this article in press as: D. Fathi, et al., All optical SRR switch using carbon nanotube composite, Optik - Int. J. Light Electron Opt. (2014), http://dx.doi.org/10.1016/j.ijleo.2014.02.039

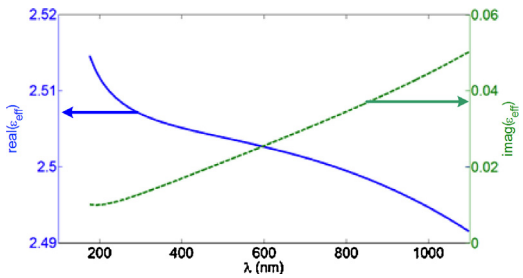

Fig. 4. The real (blue) and imaginary (green-dashed) parts of parallel effective permittivity of CNT-paraffin composite, calculated using Eq. (1). (For interpretation of the references to color in figure legend, the reader is referred to the web version of the article.)

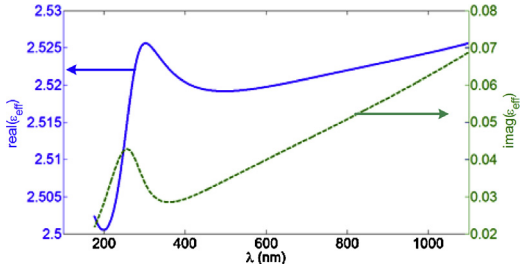

Fig. 5. The real (blue) and imaginary (green-dashed) parts of vertical effective permittivity of CNT-paraffin composite, calculated using Eq. (1). (For interpretation of the references to color in figure legend, the reader is referred to the web version of the article.)

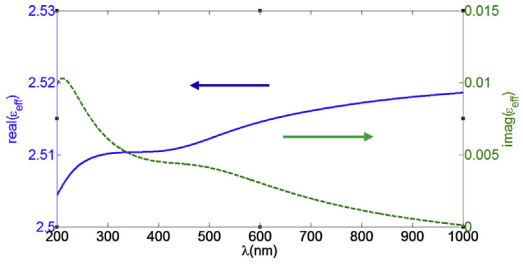

Fig. 6. The real (blue) and imaginary (green-dashed) parts of parallel effective permittivity of CNT-paraffin composite, calculated using Eq. (2). (For interpretation of the references to color in figure legend, the reader is referred to the web version of the article.)

The third order susceptibility of the CNT composite comprising identical tubules is related to the single CNT polarization by [26]

$$\chi_{\text{eff}}^{(3)} \cong \frac{f\chi_0^{(3)}}{\pi R^2} \tag{4}$$

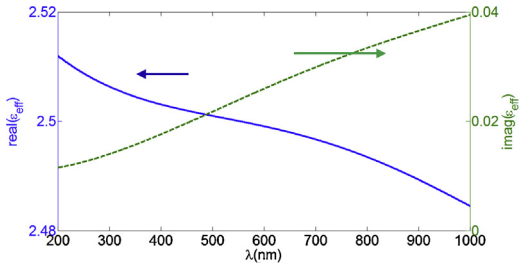

Fig. 7. The real (blue) and imaginary (green-dashed) parts of vertical effective permittivity of CNT-paraffin composite, calculated using Eq. (3). (For interpretation of the references to color in figure legend, the reader is referred to the web version of the article.)

where χ_0^3 is extracted from [17]

$$\chi_0^{(3)} \cong \frac{4}{5}\frac{(3eR)^4}{\pi^2\gamma^3}. \tag{5}$$

Using the typical values of SWCNT parameters ($R = 5.5$ Å, $\gamma = 4.46$ eV Å) we have $\chi_0^{(3)} = 3 \times 10^{-9}$ esu, and for CNTs with $R = 15$ Å and $\varepsilon_g = 0.27$ eV, we will find $\chi_0^{(3)} = 2 \times 10^{-7}$ esu. Also the radius and band gap of a SWCNT can be calculated using

$$R = \frac{a_0}{2\pi}(n_1^2 + n_2^2 - n_1 n_2)^{1/2}, \tag{6}$$

$$\varepsilon_g = \frac{2\gamma}{3R} \tag{7}$$

where $a_0 = 1.42 \times \sqrt{3}$ Å is the lattice constant of the graphite sheet.

The value of $\chi^{(3)}$ for a MWCNT is about 10^{-12} esu [27], so $\chi_{\text{eff}}^{(3)}$ for the MWCNT-paraffin composite will not be enough for switching applications. For this purpose, we have used $BaTiO_3$ instead of paraffin in the composite, which has a high $\chi_{\text{eff}}^{(3)}$ near 10^{-6} esu that has been experimentally illustrated in [19].

3.2. CNT-$BaTiO_3$ composite

The permittivity of $BaTiO_3$ is described by [28]

$$\varepsilon_c(\upsilon) = \varepsilon_{\text{LST}} + \frac{\Delta\varepsilon}{(1 - i\upsilon/\gamma)}, \tag{8}$$

where γ is the Debye frequency, $\Delta\varepsilon$ is the corresponding dielectric step and ε_{LST} is the high frequency dielectric contribution including electronic and normal lattice mode contributions and is assumed fixed 30 for all temperatures.

The complex permittivity for $BaTiO_3$ is calculated at 300 K, then the effective permittivity of CNT-$BaTiO_3$ composite is calculated using Eq. (1).

It has been shown experimentally that CNT-$BaTiO_3$ has very large effective third order susceptibility about 10^{-6} esu that is obtained by z-scan technique [19,29].

4. Discussions and simulation results

Most of the investigations in the field of CNT solid films have been focused on the imaginary part of $\chi^{(3)}$, its picosecond relaxation time, and its light emission effects. In our study, we have observed obviously the real part of third-order nonlinear susceptibility of the composite films [10,11,13].

As mentioned in Section 3.1, the value of $\chi^{(3)}$ for a MWCNT is about 10^{-12} esu based on [27], so $\chi_{\text{eff}}^{(3)}$ for the MWCNT-paraffin composite will not be enough for switching applications. For this purpose, we have used $BaTiO_3$ instead of paraffin in the composite, which has a high $\chi_{\text{eff}}^{(3)}$ near 10^{-6} esu that has been experimentally illustrated in [19].

However there is a trade-off between the MWCNT-paraffin and MWCNT-BaTiO3 composites regarding the imaginary part of $\chi_{\text{eff}}^{(3)}$. This parameter is zero for the MWCNT-paraffin composite due to the transparent region at the low frequency limit, as previously mentioned in Section 1, whereas for the MWCNT-$BaTiO_3$ composite has a nonzero value as obtained experimentally in [19]. Therefore in order to achieve a low threshold switching with a strong third order nonlinearity (the Kerr effect), we should accept a nonzero imaginary part of $\chi_{\text{eff}}^{(3)}$ which this in turn causes a slight increase in the absorption.

Please cite this article in press as: D. Fathi, et al., All optical SRR switch using carbon nanotube composite, Optik - Int. J. Light Electron Opt. (2014), http://dx.doi.org/10.1016/j.ijleo.2014.02.039

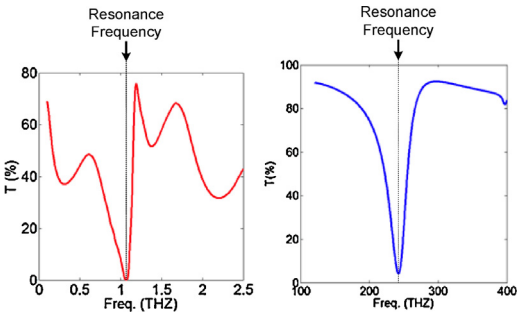

Fig. 8. The effects of geometric dimensions on the transmission coefficient and the operational frequency, for the micrometer dimensions ($a=10$, $b=2$, $c=4$ and $p=50\,\mu m$) (left) and the nanometer dimensions ($a=10$, $b=2$, $c=4$ and $p=50\,nm$) (right). (For interpretation of the references to color in figure legend, the reader is referred to the web version of the article.)

4.1. CNT-paraffin composite

For the simulation purposes, the materials in the switch structure are described by the optical properties (permittivity, permeability, susceptibility, loss), and the switching properties of the proposed structure are investigated using the FDTD[1] numerical method.

The permittivity of gold in the optical frequency range can be described by the Drud model [7]

$$\varepsilon_m = 1 - \frac{\omega_p^2}{\omega^2 + i\omega\gamma} \tag{9}$$

where $\omega_p = 2\pi \times 2.175 \times 10^{15}$ s^{-1} is the plasma frequency and $\gamma = 2\pi \times 1.95 \times 10^{13}$ s^{-1} is the damping constant.

The optical properties of CNT (MWCNT) composite layer for the simulation procedure are calculated using Eq. (1) which has been described by Fig. 5.

The surface of switch structure is illuminated by a beam from the top as shown in Fig. 1. The schematic of total structure and the related unit cell for the proposed all optical SRR switch, with $a=10$, $b=2$, $c=4$ and $p=50$ nm.

The illuminated beam is a continuous wave which is polarized in the x direction, parallel to the structure surface. Also the detector is placed at a distance far enough from the structure surface, because of avoiding the effects of diffraction at high frequencies.

The frequency of probe which is the operating frequency of switch is equal to the resonance frequency in the transmission spectrum, as shown in Fig. 8. On the other hand as this figure shows, we can adjust the operating frequency and transmission coefficient with the change of switch geometric dimensions in a wide range. As this figure shows, the resonance frequency is decreased to near 1 THz when the geometric parameters are in the range of micrometer values.

For an ideal switch, the output is zero and 100% of input when the switch is run to the off and on states respectively. In the proposed switch structure the off state is when the pump is not applied, so the output (transmission) will have the resonance frequency, as is clear from Fig. 8. The ratio of on state transmission to the off state transmission is called as the On/Off ratio (extinction ratio). At the continuation, we will investigate the effects of switch structure geometry besides the CNT composite parameters on the On/Off ratio variations.

We have changed the periodicity p to 50 nm, 60 nm and 70 nm, where the corresponding simulation results are given in Fig. 9. As shown in this figure, the operational frequency is decreased with

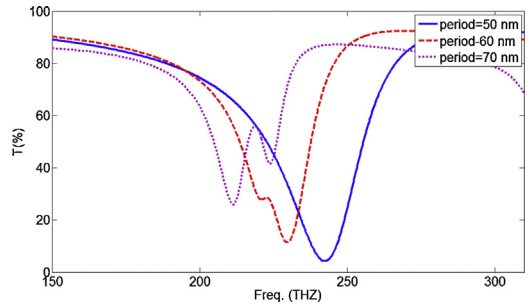

Fig. 9. The transmission coefficient versus the frequency, for various values of period; the value of CNT's volume fraction has been assumed equal to 0.01. (For interpretation of the references to color in figure legend, the reader is referred to the web version of the article.)

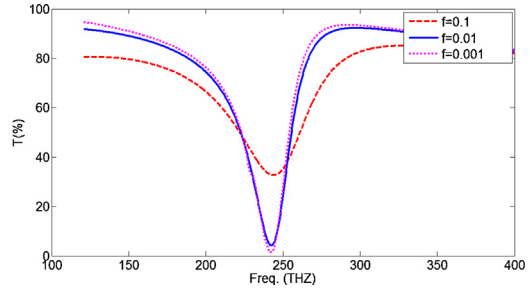

Fig. 10. The effects of CNT's volume fraction on the transmission coefficient and On/Off ratio. (For interpretation of the references to color in figure legend, the reader is referred to the web version of the article.)

the increase of periodicity, and the transmission coefficient goes to zero that means the decrease of On/Off ratio. Thus we have chosen the optimum value for the periodicity p equal to 50 nm for the switching applications.

Fig. 10 shows the effect of CNT's volume fraction (f) on the transmission coefficient variations, and also the On/Off ratio. As shown in this figure, the On/Off ratio will be increased with the decrease of f.

It should be noted that, as is cleared from Fig. 10, although the On/Off ratio has its greatest value for the volume fraction $f=0.001$, but the third order susceptibility will be decreased at this point. Thus the value of f has been considered equal to 0.01 in the simulation procedure.

Two traditional technical methods are usually used to investigate the optical properties of all optical switches. In one method which is named self switching, a continuous incident light is illuminated, while its intensity changes at a certain wavelength. In the other method, the incident light consists of two beams, one is the continuous probe beam and the other is the pulsed pump beam. In this paper, the second method has been used and the corresponding nonlinear response for the switch structure has been obtained, as shown in Fig. 11. This figure shows the red shift of transmission spectrum for two cases of $\Delta\varepsilon = 0.1, 0.2$.

It is necessary to note that, the operating frequency of switch is determined by the low power signal (probe) containing the input optical information, which in turn does not cause any nonlinear effects. On the other hand, for achieving the On/Off switch application, the strong third order nonlinear effect is required which this duty is performed by applying the high power signal (pump). For this purpose, the pump should be operated in the lower frequency range, which is neither near the infrared nor the optical wavelengths.

As cleared from Fig. 11, when $\Delta\varepsilon$ is increased to 0.2, an obvious red shift will be occurred in the transmission coefficient spectrum. This causes an increase of output signal (transmission; %) up to

[1] Finite Difference Time Domain.

Please cite this article in press as: D. Fathi, et al., All optical SRR switch using carbon nanotube composite, Optik - Int. J. Light Electron Opt. (2014), http://dx.doi.org/10.1016/j.ijleo.2014.02.039

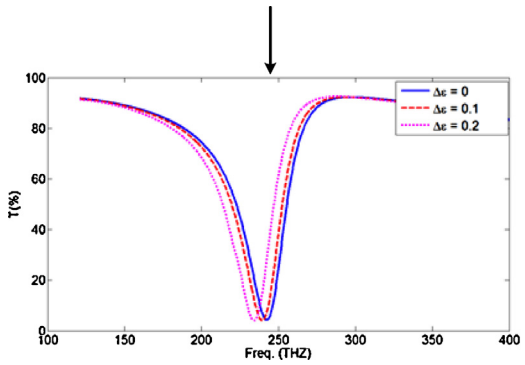

Fig. 11. The transmission coefficient versus the frequency (wavelength), for various values of $\Delta\varepsilon$; the red shift occurs with $\Delta\varepsilon = 0.1, 0.2$. (For interpretation of the references to color in figure legend, the reader is referred to the web version of the article.)

50% that means on state. For achieving this situation, the required $|E|^2 = 35.8\ \mathrm{kV}^2$ per unit cell is calculated from

$$\varepsilon_d = \varepsilon + \chi^3 |E|^2. \tag{10}$$

The corresponding pump power $|E|^2$ calculated above is a large value, because of the weak third order susceptibility of MWCNT-paraffin composite. Therefore, we have changed the composite to MWCNT-$BaTiO_3$, which the corresponding simulation results are presented at the following section.

4.2. CNT-$BaTiO_3$ composite

For obtaining a large third order nonlinear susceptibility $\chi^{(3)}$ and small relaxation time of photo carriers, the CNT-$BaTiO_3$ composite has been used in this section, and the simulation results have been obtained.

Fig. 12 shows the transmission coefficient spectrum versus the wavelength (frequency) for various values of $\Delta\varepsilon$. The blue curve (solid line) in this figure shows the transmission coefficient variations in the steady state where the pump power is not applied. We suggest that the probe frequency is tuned near 870 THz where the state of switch is normally off. The transmission spectrum is also shown in Fig. 12 when the pump is applied, for the values of $\Delta\varepsilon = 0$, 1, 3, 4. As is cleared from this figure, an obvious red shift will be occurred in the transmission spectrum for $\Delta\varepsilon = 4$, that causes an increase of output to near 95%. This is because the required pump power $|E|^2$ will be equal to $7.16\ \mathrm{mV}^2$ per unit cell, using Eq. (10), with $\chi^{(3)} = 10^{-6}$ esu.

It should be noted that, all the data used from some references (including the mentioned above) in our simulations are experimental, where we have cited to these references through the text. For example, the CNT composite permittivity is calculated using the Maxwell–Garnett and Brugman methods, which have been verified experimentally in references [23,24].

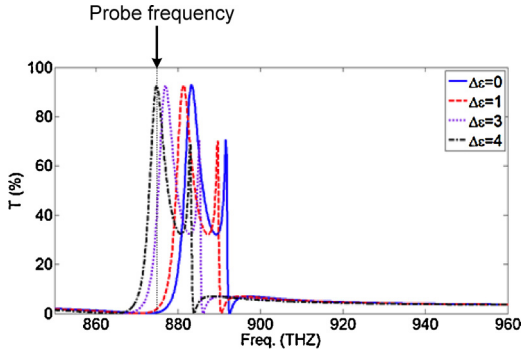

Fig. 12. The transmission coefficient spectrum versus the frequency, for various values of $\Delta\varepsilon$. (For interpretation of the references to color near the citation of this figure, the reader is referred to the web version of the article.)

5. Conclusions

In this paper, we have proposed and numerically investigated a new nanostructure for an all optical SRR metamaterial switch, based on MWCNT composite as the nonlinear layer. The obtained results demonstrate that, the switching response can be tuned from nearly zero to one, which this gives an excellent On/Off ratio. Also, we have used the CNT-$BaTiO_3$ composite with a high nonlinear effect that causes a low threshold power for switching, nearly $7.16\ \mathrm{mV}^2$ per unit cell.

Another advantage of the purposed structure is using the CNT based composites, which not only gives strong nonlinear properties but also achieves a good feasible situation regarding the fabrication possibilities.

Finally, the proposed structure has a high potential to be used in all optical integrated photonic circuits.

References

[1] K.Y. Kim, J.-H. Lee, Y.K. Cho, H.-S. Tae, Electromagnetic wave propagation through doubly dispersive subwavelength metamaterial hole, Opt. Express 13 (2005) 3653–3665.
[2] X. Huang, D. Ye, S. Xiao, J. Huangfu, Z. Wang, L. Ran, et al., Fractal plasmonic metamaterials for subwavelength imaging, Opt. Express 18 (2009–2010) 10377–10387.
[3] A. Alù, N. Engheta, Plasmonic and metamaterial cloaking: physical mechanisms and potentials, J. Opt. A: Pure Appl. Opt. 10 (2008) 093002.
[4] M. Kafesaki, I. Tsiapa, N. Katsarakis, T. Koschny, C. Soukoulis, E. Economou, Left-handed metamaterials: the fishnet structure and its variations, Phys. Rev. B 75 (2007) 235114.
[5] B. Wang, J. Zhou, T. Koschny, C.M. Soukoulis, Nonlinear Properties of Split-Ring Resonators, 2008 arXiv:0809.4045.
[6] H.T. Chen, W.J. Padilla, J.M.O. Zide, A.C. Gossard, A.J. Taylor, R.D. Averitt, Active terahertz metamaterial devices, Nature 444 (2006) 597–600.
[7] Y. Gong, Z. Li, J. Fu, Y. Chen, G. Wang, H. Lu, et al., Highly flexible all-optical metamaterial absorption switching assisted by Kerr-nonlinear effect, Opt. Express 19 (2011) 10193–10198.
[8] Y. Shen, G.P. Wang, Optical bistability in metal gap waveguide nanocavities, Opt. Express 16 (2008) 8421–8426.
[9] S. Iijima, Helical microtubules of graphitic carbon, Nature 354 (1991) 56–58.
[10] Y. Zhu, H.I. Elim, Y.L. Foo, T. Yu, Y. Liu, W. Ji, et al., Multiwalled carbon nanotubes beaded with ZnO nanoparticles for ultrafast nonlinear optical switching, Adv. Mater. 18 (2006) 587–592.
[11] A. Martinez, S. Uchida, Y.-W. Song, T. Ishigure, S. Yamashita, Fabrication of carbon nanotube poly-methyl-methacrylate composites for nonlinear photonic devices, Opt. Express 16 (15) (2008) 11337–11343.
[12] K. Chow, S. Yamashita, Four-wave mixing in a single-walled carbon-nanotube-deposited D-shaped fiber and its application in tunable wavelength conversion, Opt. Express 17 (2009) 15608–15613.
[13] V. Scardaci, A. Rozhin, F. Hennrich, W. Milne, A. Ferrari, Carbon nanotube–polymer composites for photonic devices, Phys. E: Low-dimens. Syst. Nanostruct. 37 (2007) 115–118.
[14] P.R. Bandaru, C. Daraio, S. Jin, A. Rao, Novel electrical switching behaviour and logic in carbon nanotube Y-junctions, Nat. Mater. 4 (2005) 663–666.
[15] T. Hasan, Z. Sun, F. Wang, F. Bonaccorso, P.H. Tan, A.G. Rozhin, et al., Nanotube–polymer composites for ultrafast photonics, Adv. Mater. 21 (2009) 3874–3899.
[16] Y.-C. Chen, N. Raravikar, L. Schadler, P. Ajayan, Y.-P. Zhao, T.-M. Lu, et al., Ultrafast optical switching properties of single-wall carbon nanotube polymer composites at 1.55 μm, Appl. Phys. Lett. 81 (2002) 975–977.
[17] V.A. Margulis, T. Sizikova, Theoretical study of third-order nonlinear optical response of semiconductor carbon nanotubes, Phys. B: Condens. Matter 245 (1998) 173–189.
[18] H. Bao, X. Ruan, T.S. Fisher, Optical properties of ordered vertical arrays of multi-walled carbon nanotubes from FDTD simulations, Opt. Express 18 (2010) 6347–6359.
[19] G. Lu, B. Cheng, H. Shen, Y. Chen, T. Wang, Z. Chen, et al., Large optical third-order nonlinearity of composite thin film of carbon nanotubes and $BaTiO_3$, Chem. Phys. Lett. 407 (2005) 397–401.
[20] D. Schurig, J. Mock, D. Smith, Electric-field-coupled resonators for negative permittivity metamaterials, Appl. Phys. Lett. 88 (2006), 041109-041109-3.
[21] W. Cai, V.M. Shalaev, Optical Metamaterials: Fundamentals and Applications, Springer, New York, 2010.

Please cite this article in press as: D. Fathi, et al., All optical SRR switch using carbon nanotube composite, Optik - Int. J. Light Electron Opt. (2014), http://dx.doi.org/10.1016/j.ijleo.2014.02.039

[22] Y. Liu, F. Qin, F. Zhou, Z.Y. Li, Ultrafast and low-power photonic crystal all-optical switching with resonant cavities, J. Appl. Phys. 106 (2009), 083102-083102-9.
[23] T. Xiao, H.L. Yang, G.P. Zhang, The influence of carbon nanotube structure on complex permittivity and determination of filler density by microwave techniques, J. Appl. Phys. 110 (2011) 024902.
[24] E.A. Taft, H. Philipp, Optical properties of graphite, Phys. Rev. 138 (1965) A197.
[25] V.A. Margulis, Theoretical estimations of third-order optical nonlinearities for semiconductor carbon nanotubes, J. Phys.: Condens. Matter 11 (1999) 3065.
[26] A. Nemilentsau, G.Y. Slepyan, A. Khrutchinskii, S. Maksimenko, Third-order optical nonlinearity in single-wall carbon nanotubes, Carbon 44 (2006) 2246–2253.
[27] Z. Wang, C. Liu, H. Xiang, Z. Li, Q. Gong, Y. Qin, et al., Ultrafast third-order nonlinear optical response of two soluble multi-wall carbon nanotubes, J. Phys. D: Appl. Phys. 37 (2004) 1079.
[28] J. Hlinka, T. Ostapchuk, D. Nuzhnyy, J. Petzelt, P. Kuzel, C. Kadlec, et al., Coexistence of the phonon and relaxation soft modes in the terahertz dielectric response of tetragonal $BaTi_3$, Phys. Rev. Lett. 101 (2008) 167402.
[29] L. Guo-Wei, C. Bo-Li, S. Hong, C. Yu-Jin, Z. Yue-Liang, C. Zheng-Hao, et al., Optical properties of carbon nanotubes and $BaTiO_3$ composite thin films, Chin. Phys. 15 (2006) 1815.

Please cite this article in press as: D. Fathi, et al., All optical SRR switch using carbon nanotube composite, Optik - Int. J. Light Electron Opt. (2014), http://dx.doi.org/10.1016/j.ijleo.2014.02.039